Microalgae and bacteria dynamics in high rate algal ponds based on modelling results: long-term application of BIO_ALGAE model

Alessandro Solimeno and Joan García*

GEMMA – Group of Environmental Engineering and Microbiology, Department of Civil and Environmental Engineering, Universitat Politècnica de Catalunya-BarcelonaTech, c/Jordi Girona, 1-3, Building D1, E-08034, Barcelona, Spain.

*Corresponding author. Tel: +34 93 401 6464; fax 34 93 401 73 57.

E-mail address: solimeno.ale@gmail.com (A. Solimeno).

1. Introduction

High rate algal pond (HRAP) technology for wastewater treatment was developed in California by Prof. Oswald in the 1950s as an alternative to conventional waste stabilisation ponds (WPS) (Oswald and Gotaas, 1957). The smaller footprint of HRAP systems coupled with the benefit of production of valuable products (e.g. biofuels, bioplastics) from microalgae feedstock makes them more attractive over WPS (García et al. 2000a; Faleschini et al. 2012).

HRAPs are based on microalgae and bacteria interactions in wastewater exposed to light. Microalgae photosynthesis provides oxygen necessary for the degradation of organic compounds present in wastewater by aerobic bacteria. During bacterial oxidation of organic matter, carbon dioxide (CO_2) is produced and is available for both photosynthesis and nitrification (Oswald 1988). The many processes that occur in microalgae-bacteria systems are quite difficult to control (García et al. 2006; Awuah 2006; Fuentes et al. 2016). Moreover, these processes depend on ever-changing environmental variables such as solar radiation and temperature.

Although these systems have been studied for many years, still today the physical, chemical and biochemical reactions that occur in microalgae-bacteria systems are less well known than processes in conventional technologies, such as activated sludge. In fact, it is still very challenging to understand which are the main factors affecting microorganisms growth and production (i.e. microalgae and bacteria), and how their interactions affect the relative proportion of microorganisms. Recently, variations of biomass production over a year in pilot-scale HRAPs were experimentally evaluated by Mehrabadi et al. (2016). These authors observed that changes in microalgae concentration were clearly linked to seasonal fluctuations in temperature and light intensity in the absence of nutrient limitation. Other studies have shown that HRAP operating conditions play an important role on biomass composition, and of course the efficiency for removing pollutants. In a study conducted by Park and Craggs (2011), hydraulic retention time (HRT) clearly influenced microalgae proportion dynamics. A low hydraulic retention time (HRT, 2 days) yielded much more microalgae biomass than bacteria (80% of average of total biomass), while high HRT (8 days) had lower microalgae proportion (56% of average of total biomass). Note that these authors estimated microalgae proportion indirectly by measurements of chlorophyll-a concentration. At present time is not trivial to have a direct measure of microalgae and bacteria proportion in such mixed cultures.

Mathematical models have proven to be useful tools to understand and optimize the functioning of biological wastewater treatment systems, including microalgae-bacteria systems (Park and Craggs 2011; Zhou et al. 2014). Solimeno et al. (2017a) developed the mechanistic BIO_ALGAE model to understand the internal functioning of complex microalgae-bacteria systems. One relevant feature of the model is that it allows microbial biomass concentration prediction, and thus evaluation of the relative proportions of microorganisms (Solimeno et al. 2015; 2017a; 2017b).

The River Water Quality Model 1 (RWQM1) (Reichert et al. 2001) and the ASM3 model (Iacopozzi et al. 2007) (International Water Association, IWA) were selected to describe microalgae and bacteria processes, respectively. Inorganic carbon as a limiting substrate for the growth of microalgae is one of the major innovative processes of BIO_ALGAE. Moreover, temperature, photorespiration, pH dynamics, solar radiation, light attenuation and rate of transfer of gases to the atmosphere are considered main limiting factors for microalgae growth. BIO_ALGAE was implemented in the COMSOL Multiphysics^{TM} software, which solves differential model equations using the finite elements method (FEM). This model was previously calibrated and validated with high quality experimental data from duplicated pilot HRAPs receiving real wastewater (Solimeno et al. 2017a). Calibration was conducted by adjusting the following 6 parameters selected after a Morris's sensitivity analysis: 3 parameters related to microalgae and heterotrophic bacteria specific growth rate and decay of heterotrophic bacteria, and 3 parameters related to the transfer of gases to the atmosphere. These parameters were carefully calibrated and validated in our previous work comparing field data over 4 intensive days of experiments to predict daily fluctuations of the components in the ponds, and the relative proportions of microalgae and bacteria in a short-time scale. A long-term validation is essential to demonstrate (1) the capacity of the model to predict seasonal variations of microalgae and bacteria biomass, and (2) the effect of different HRT operating strategies on the HRAP performance, biomass production and biomass proportions.

Therefore, the aim of the present study is to validate the BIO_ALGAE model with experimental data from a pilot HRAP gathered during two different seasons (summer and winter), and operating at different HRT (4 and 8 days). Moreover, the potential of the model is demonstrated by means of practical study cases in which microalgae production, the relative proportion of microalgae and bacteria, and the ammonium removal efficiency were compared over an annual cycle. Hence, the purpose of this study was to study HRT and season effects on HRAP performance: microalgae production, the relative proportion of microalgae to bacteria, and ammonium removal efficiency.

2. Material and methods

2.1. Experimental data

The data used for simulations were obtained from previous studies conducted by the authors in a pilot HRAP (García et al. 2000a; 2002). A detailed description of the system can be found in these studies. In brief, the pilot HRAP was installed outdoors on the roof of the Group of Environmental Engineering and Microbiology (GEMMA) building (Universitat Politècnica de Catalunya-BarcelonaTech, Barcelona, Spain, latitude: 41° 23' 24.7380" N; longitude: 2° 9' 14.4252" E). The data used in this study were collected from July 1993 to October 1993 (Period I), and from November 1993 to February 1994 (Period II), corresponding to low and high HRT of the pilot (4 and 8 days, referred as $HRAP_{4d}$ and $HRAP_{8d}$, respectively). In practice, low HRT is used in warmer periods (summer-autumn), while high HRT are used in colder periods (autumn-winter) to maintain stable contaminant removal efficiencies (García et al. 2006).

The pilot HRAP was a typical race track built in PVC with a water surface area of 1.54 m^2 and a water depth of 0.34 m, and a nominal volume of 0.47 m^3 (Fig. 1). A single paddlewheel was set to provide a rotational speed of 5 rpm and a mid-channel velocity of approximately 9 cm s^{-1}, avoiding biomass settling. HRAP received primary treated urban wastewater from a near street sewer, which was continuously pumped to the pond. Primary treatment was conducted in a 0.5 m^3 storage tank. HRT of the HRAP was controlled by wastewater flow.

Samples of HRAP influent, HRAP mixed liquor (identical to HRAPs effluent, because of almost perfect complete mixing) were taken once a week, at 2:00 PM ±1 hour. Description of the methods used for analyses can be found in García et al. (2000a, 2002). Water temperature, pH and DO (dissolved oxygen) were measured weekly, at 9:00 AM ±1 and at 2:00 PM ±1 hour. Maximum and minimum water temperature and irradiance recorded over the two periods investigated are shown in Table 1a.

Irradiance and air temperature were obtained from a nearby meteorological station.

2.2. Model implementation

Simulations were conducted using the BIO_ALGAE model. A detailed description of the components, the biokinetic processes, and the chemical and physical equations were presented in our previous works (Solimeno et al. 2015; 2017a; 2017b). To simplify presentation of the simulation results, Tables S1 and S2 in Supplementary Material (SM) present the biokinetic processes and the matrix of stoichiometric parameters. Values of biokinetic, physical and chemical parameters are shown in SM, Tables S3-S4. Mathematical expressions of the stoichiometric coefficients of each process are also shown in SM, Table S5.

The model was implemented in COMSOL Multiphysics^{TM} v5.1 software. A simplified 1D domain was used to represent a vertical section of the pilot HRAP. Assuming that each section behaves similarly due to perfect mixing of culture medium, this reasonable simplification allowed a reduction of computational cost. The culture was mixed with the paddlewheel, which ensured almost complete stirred reactor behaviour due to the small volume of the high rate pond in relation with the big size of the blades of the paddlewheel.

According to the Beer-Lambert law, irradiance decays exponentially as it passes through the HRAP mixed liquor. Therefore, a depth-averaged irradiance I [µmol m^{-2} s^{-1}] was used to represent irradiance at any point of the pond (Solimeno et al. 2017a). The penetration pathway corresponded to the depth of the HRAP (0.3 m).

2.3. Validation procedure

BIO_ALGAE includes 93 parameters describing microalgae, bacteria, physical and chemical processes (Tables S3-S4, SM). Most of these parameters were obtained from the existing RWQM1 [15], ASM1, and ASM3 models (Henze et al. 2000; Iacopozzi et al. 2007). Parameters related to temperature, photorespiration, carbon limitation and light attenuation were obtained from other literature cited in SM (Table S3-S4). Morris uncertainty method was applied in our previously work (Solimeno et al. 2016; 2017a) to identify the parameters which had the greatest influence on the simulation response (Morris 1991). Results from our previous works have shown that the values of maximum growth rate of microalgae (μ_{ALG}), the maximum growth rate and the decay of heterotrophic bacteria (μ_H and $k_{death,H}$) and the parameters related to the transfer of gases to the atmosphere ($K_{a,O2}$, $K_{a,CO2}$ and $K_{a,NH3}$), were very sensitive and need to be calibrated in each application of the model (Solimeno et al. 2015; 2016).

In the present work, these parameters were set based on a previous calibration and validation effort using experimental data from duplicate HRAPs located at the Delhi wastewater pond treatment plant (California) during 4 days of experiments (Solimeno et al. 2017a). Results of this earlier effort indicated that the model was able to match experimental data accurately. Influent HRAP average concentrations observed in each experimental period were used as constant input values to run simulations (Table 1b). Influent concentrations of nitrate and nitrite were lower than the analytical method's detection limit and therefore considered to be zero in the input for the model. Ammonium nitrogen comprised almost 90% of dissolved Kjeldahl nitrogen (García et al. 2000a), and therefore the concentration of organic nitrogen present in the influent wastewater was omitted from the model.

Fractions of influent chemical oxygen demand (COD) were estimated from rational values for primary effluents in Activated Sludge Model No1 (ASM1) (Henze et al. 2000). Accordingly, the proportion of each fraction was defined as: 22% readily biodegradable soluble organic matter (S_S), 50% slowly biodegradable particulate organic matter X_S, 10% inert soluble organic matter (S_I), 8% inert particulate organic matter (X_I) and 10% heterotrophic bacteria (X_H). In the present work microalgae and bacteria biomass are transformed from COD to total suspended solids (TSS) assuming a ratio COD/TSS = 0.80 (Khorasandi et al. 2014) in order to compare experimental and simulation results. Note that some authors apply different ratios, for example, Von Sperling (2007) found values of 1–1.5 in waste stabilization pond effluents.

The concentrations of components in the mixed liquor of the HRAP measured at the beginning of the two experimental periods are shown and described in Table 2. Unfortunately, the concentration of each particulate component (X_{ALG}, X_S, X_I, $X_{H,}$ X_{AOB} and X_{NOB}) in the mixed liquor was not known (where X_{ALG} is microalgae concentrations and X_{AOB}, X_{NOB} are ammonium and nitrite oxidizing bacteria, respectively).

Therefore, initial ratio of X_{ALG}, X_S, X_I, $X_{H,}$ X_{AOB} and X_{NOB} concentrations were quantified from initial TSS value (from M1 pond) based on previous simulation tests.

This assumption also provided an initial relationship between pH, dissolved oxygen, and nutrients (i.e. nitrogen and carbon).

Validation was performed by comparing measured data with simulation patterns using graphs of the two periods (with different HRT). Tested components during validation were: pH, dissolved oxygen (S_{O2}), bicarbonate (S_{HCO3}), ammonium (S_{NH4}), nitrate (S_{NO3}), nitrite (S_{NO2}) and TSS. Model data were compared to experimental data by the root mean square error (RMSE).

2.4. Case studies: relative proportion of microalgae and bacteria, and biomass production forecasting over a year cycle

Practical case studies were conducted to evaluate the variations in biomass production and the relative proportion of microalgae and bacteria over a year cycle (from January to December). The experiments were conducted over an annual cycle in order to investigate the influence of different HRT operating strategies and seasonal variations of temperature and irradiance on the relative proportion of microalgae and bacteria, and biomass production over a year cycle.

In these studies, we simulated the evolution of microalgae, bacteria and TSS concentrations starting from the initial mixed liquor concentration used for the validation of the model at the beginning of the month of February, and using average influent wastewater concentration showed in Table 3. In addition, ammonium and ammonia concentration (S_{NH4}+S_{NH3}) were evaluated as indicators of removal efficiency because they are very sensitive to changes in the environmental conditions in HRAPs. According to European standard (European Council 1991), HRAP performance is suitable when the concentration of ammonium and ammonia in the effluent is lower than 10 gN m^{-3}. Three scenarios were evaluated: 1) the HRAP operating at 4-day HRT ($HRAP_{4d}$) over the whole year; 2) the HRAP operating at 8-day HRT ($HRAP_{8d}$) over the whole year, and 3) the HRAP operating with different HRT, from April to September at 4-day HRT and from October to March at 8-day HRT ($HRAP_{8\text{-}4\text{-}8d}$).

The standard method of changing HRT during different seasons to maintain removal efficiency was investigated according to the results of previous experimental research carried out in Barcelona (García et al. 2000b). Water temperature data taken weekly at 9:00 AM ±1 hour, and at 2:00 PM ±1 hour measured over the one-year monitoring period, and irradiance data from the meteorological station of physical department of University of Barcelona (around 2 km far from the pilot HRAP) were used to run simulations for study cases.

3. Results and discussion

In this section, first of all, air temperature and irradiance changes over the course of all experiments were showed in Fig.2. As can be seen temperature and irradiance were greater in Period I than in Period II. Also in Period I the general trend of temperature and irradiance was a progressive decrease from July to October, while changes in Period II were more subtle. Following, performance assessment of the model in predicting experimental data under different HRTs were presented.

3.1. HRAP$_{4d}$ validation (Period I)

Figure 3 shows the results of the validation in the HRAP$_{4d}$ from July to October. Simulations were able to follow measured pH and S_{O2} trends during the whole experimental period (Fig. 3a-b). As can be seen, both variables have a daily oscillations pattern due mostly to microalgae photosynthetic activity. This trend is in agreement with previous simulation results obtained during calibration in our previous study (Solimeno et al. 2017a), and also with previous experimental studies (García et al. 2006). Simulated daily minimum and maximum values were generally higher and lower than values measured at 9:00 AM and 2:00 PM, respectively, because the peaks of microalgae activity do not necessary coincide with these hours. From simulations, pH values ranged from 7.4 to 10.1, with an average of 8.5, while S_{O2} concentration ranged from 0 $gO_2\ m^{-3}$ to 28.1 $gO_2\ m^{-3}$, with an average of 11.2 $gO_2\ m^{-3}$. It is possible to see how at the end of this period daily fluctuations of pH and S_{O2} were slightly smoother than at the beginning of the study. At night, S_{O2} concentration decreased to be usually less than 5 $gO_2\ m^{-3}$, and even in some few cases almost 0 due to the lack of photosynthesis and the intense microbial respiration.

Simulations followed the trend observed for measured S_{HCO3}, S_{NH4}, S_{NO3} and S_{NO2} with different degree of success (Fig. 3c-f). Simulated S_{HCO3} and S_{NH4} curves matched quite well with the experimental data, and present a clear oscillation pattern mostly related to photosynthesis, with lower values of both variables during daytime. Microalgae grow during daytime using bicarbonate as carbon source, and subsequently pH raises favoring conversion of ammonium to ammonia, which is lost in part through volatilization. Moreover, microalgae uptake also contributes to ammonium decrease during daytime. These trends are also in agreement with simulation results carried out during calibration in our previous study (Solimeno et al. 2017a), and with previous experimental studies (García et al. 2006). Daily fluctuations of S_{HCO3} and S_{NH4} tend to soften towards the end of Period I (Fig 3c-d); the same pattern was observed for pH and S_{O2}. This is indicative of a lower photosynthetic activity due to decrease of incident irradiance and temperature.

As can be seen in Figure ~~S2d~~3d, S_{NH4} simulated concentrations were relatively low and constant during July and August (the first 60 days), and increased from mid-September, corresponding with the decrease in incident irradiance and temperature. This also corresponds with the lower overall microalgae activity. Higher values of S_{NO3} and S_{NO2} were observed towards the end of the period, when S_{NH4} concentration was also higher. The model was able to simulate these trends described for S_{NO3} and S_{NO2} quite well, and it can be seen that photosynthesis influences these compounds much less due to the much lower daily oscillation trends.

Simulated TSS concentration fits experimental data with a good degree of accuracy (Fig. 3g). The model is able to predict curves of microalgal (X_{ALG}) and bacterial biomass concentrations (X_H, X_{AOB} and X_{NOB}) (Fig. 3h-i). Simulated X_{ALG} concentration exhibits an oscillation trend, reflecting microalgae growth during daytime (crest) and decay at night (trough); heterotrophic bacteria concentration simulations do not exhibit this pattern. During the period, X_{ALG} gradually decreased, following the decreases in irradiance and temperature, while X_H remained relatively constant. In July and August (the first 60 days), high irradiance and temperature produced a high photosynthetic activity, which at the same time produced high daily peaks of S_{O2} (often greater than 25 gO_2 m^{-3}). Concentrations of DO in the culture above 250% air saturation (22.6 gO_2 m^{-3}) can dangerously inhibit microalgae activity (Costache et al. 2013). Subsequently these peaks seem to limit microalgae growth due to photorespiration. As can be seen in Figure 4a, the photorespiration factor ($f_{PR}(O_2)$) reduced microalgae growth from 20 to 40% (values of the factor from 0.8 to 0.6, respectively). Thus, excess of oxygen caused less microalgae production that could had been avoided with improved oxygen transfer to the atmosphere. A detailed description of photorespiration factor is provided in SM. Also the drop in temperature from mid-September (day 65) had impact on X_{ALG}, causing a reduction of growth between 10 to 20% through the thermic photosynthetic factor ($f_{T,FS}$) (Figure 4b) (see also SM for a detailed description of this factor).

Nitrifying bacteria (X_{AOB} and X_{NOB}) concentration was very low in comparison to X_H. This observation has already been reported in previous simulation studies, and for other types of wastewater treatment systems (Krasnits et al. 2009; Samsó and García 2013; Solimeno et al. 2017a)

Altogether, simulation results have predicted that much of the organic matter present in the mixed liquor corresponds to X_{ALG} (55% in average of TSS) and X_H (26% in average of TSS). X_{AOB} and X_{NOB} are comparatively very low (0.35%), and the remaining solids are attributable to X_S (5.5%) and X_I (13.2%).

3.2. HRAP$_{8d}$ validation (Period II)

Figure 5 shows the results of the validation in the HRAP$_{8d}$ from November to February. Again, the model exhibited the oscillation trend for pH and S_{O2} during the whole experimental period (Fig. 5a-b), with lower values in comparison to Period I. The degree of model fit was slightly lower than in Period I. Simulation results indicated that pH values ranged from 7.2 to 9.6, with an average of 8.1, while S_{O2} concentrations ranged from 0.9 gO_2 m^{-3} to 20 gO_2 m^{-3} with an average of 11 gO_2 m^{-3}. Daily fluctuations of pH and S_{O2} were shorter than in Period 1. In comparison to Period 1, nighttime S_{O2} concentration rarely decreased to below 5 gO_2 m^{-3} due to the lower overall microbial respiration and lower temperature (which increased transfer from the atmosphere to the mixed liquor).

Model validation results for HRAP$_{4d}$conditions were comparable for S_{HCO3}, S_{NH4} and S_{NO2} data. Conversely, simulated S_{NO3} concentration did not match experimental data as closely as in Period I. Simulated S_{HCO3} and S_{NH4} exhibited the oscillation pattern already mentioned in Period I, but with shorter daily fluctuations, similar to the last part of Period I (when irradiance and temperature decreased). This is indicative of a lower overall photosynthetic activity in comparison to Period I. Much higher values of S_{NO2} were observed towards the end of Period II, when S_{NH4} was higher.

As can be seen in Figure 5g, the model was able to simulate TSS concentration with a good degree of accuracy. With respect to HRAP$_{4d}$, predicted concentrations of TSS, X_{ALG}, X_H, X_{AOB} and X_{NOB} were lower than the data (although HRT was higher than in Period I) (Fig. 5g-i). Lower X_{ALG} ~~–~~concentration was mostly due to the temperature (and to irradiance to a lesser extent). Figure ~~S4j~~ 5j shows reduction of growth from 10 to 30% through the thermic photosynthetic factor ($f_{T,FS}$), and as can be seen was much lower in Period II than in Period I (compare with Fig. 4b). Although COD influent in Period II (195 ± 50 g O_2 m^{-3}) was slightly higher than the in Period I (180 ± 84 gO_2 m^{-3}), X_H concentration was lower due to the lower temperature. Bacteria thermal factor ($f_{T,MB}$) shows reduction of X_H growth from 40 to 60% (Fig. 5j).

X_{ALG} was higher (58% in average of TSS) than X_H (22% in average of TSS). X_{AOB} and X_{NOB} biomass was comparatively much lower (2.4%), but still higher than the estimated value for Period I. The remaining solids were attributable to X_S (6%) and X_I (11.6%).

A comparative evaluation indicates that HRT should be high enough to guarantee treatment performance and to prevent wash-out effects (Larsdotter 2006). Simulation results indicated that a higher HRT during the winter would probably be necessary than during the summer as result of the lower growth rate of microalgae as well as bacteria.

Table 4 presents the RMSE values obtained comparing the experimental data with the model simulations obtained from the validation of the model for each period investigated. Values of RMSE near zero indicate that the model fits experimental data well [28]. RMSE values for pH, dissolved oxygen, bicarbonate, nitrogen species and total suspended solids are in good accordance with the RMSE values calculated during the calibration of the model (Solimeno et al. 2017a).

3.3. Study case: relative proportion of microalgae and bacteria, biomass production and ammonium removal efficiency of $HRAP_{4d}$ over a year cycle.

In this case study, the relative proportion of microalgae and bacteria, and the production of microalgae are predicted with the HRAP operating continuously with 4-day HRT. Figure 6a presents simulations of X_{ALG}, X_H and TSS concentrations. X_{ALG} was different between seasons, being lower in colder months (from November to March) and higher in warmer months (from April to October). The photorespiration effect limited microalgae growth during the warmer months, keeping the concentrations around 225 gTSS m^{-3}. X_H concentration was quite constant over the year due to the constant influent wastewater features. As can be seen from Figure 6b, microalgae proportion with respect to bacteria increased from April to October up to 60-75% and dropped down to 27-33% from November to March. Trends suggested by these results are in accordance with the experimental studied by Park and Craggs (2011). In their study, the proportion of X_{ALG} (estimated indirectly) in the microalgae-bacteria biomass of an HRAP operating at 4-day HRT with CO_2 addition in summer was estimated to be around 80%.

X_{ALG} and TSS production are shown in Figure 6c. Predictions indicate that during the warmer month with a 4-day HRT, it is possible to reach up to 20 gTSS $m^{-2}d^{-1}$ of X_{ALG} production. Although pH values in summer are very high (> 9, Fig. 7a), the model indicates that microalgae are not carbon limited (carbon Monod function= 0.99). Furthermore, S_{O2} in excess limits microalgae growth through photorespiration (average f_{PR} (S_{O2}) = 0.62 in summer) (Fig. 7a).

Ammoniacal nitrogen concentration (sum of ammonium plus ammonia S_{NH4}+S_{NH3}, from now on "ammonium") was used as an indicator of efficiency of HRAP treatment wastewater. As can be seen in Figure 7b, S_{NH4} has a clear seasonal pattern. In colder months, only approximately an average of 40% of the influent (49 g N_NH_4 m^{-3}) is removed, while in warmer months average removal rate goes up to 90%.

3.4. Study case: relative proportion of microalgae and bacteria, biomass production and ammonium removal efficiency of $HRAP_{8d}$ over a year cycle.

In this case study, the HRAP is continuously operated with 8-day HRT. Figure 8a presents simulations of X_{ALG}, X_H and TSS concentrations. X_{ALG} changed less over the year in comparison to the $HRAP_{4d}$. X_H concentrations were quite constant over the year, and had similar concentrations to $HRAP_{4d}$. As can be seen from Figure 8b, microalgae proportion in comparison to bacteria was higher from April to October (76-78%), and slightly dropped down to 65-68% from November to March. In this case study, X_{ALG} were more abundant than X_H over the entire year. These trends are not in agreement with the experimental study by Park and Craggs (2011), where the proportion of microalgae (estimated indirectly) of an HRAP operating at 8-days HRT with CO_2 addition in summer was around 55.6%, much lower than in a 4-day HRT. Park and Craggs (2011) indicated that microalgae growth was limited due to low light availability in the pond. Irradiance was attenuated by the high biomass concentration up to 430 g VSS m^{-3}, while in our numerical experiment the biomass concentration in term of TSS is maintained below of 400 g TSS m^{-3}.

X_{ALG} and TSS production are compared in Figure 8c. Predictions indicate that with an 8-day HRT, it is possible to reach up to 10.6 g TSS $m^{-2}d^{-1}$ of X_{ALG} production in warmer months, which resulted 50% lower than X_{ALG} production predicted in 4-day HRT. In this case study pH is also very high in summer (> 9, Fig. 9a), however the model indicates that microalgae are not carbon limited. Again, S_{O2} in excess limits microalgae growth through photorespiration (average f_{PR} (S_{O2}) = 0.42 in summer) (Fig. 9b). Excess of S_{O2} was much higher than $HRAP_{4d.}$ With an 8-day HRT the mass influent organic matter concentration in the pond is reduced, therefore oxygen demand by X_H to oxidize organic matter is lower than oxygen produced by microalgae during the photosynthesis due to the high concentration of X_{ALG} (260 gTSS m^{-3}.in summer). As can be seen in Figure 9c, the model prediction indicated that average ammonium removal rate goes up to 98% of the influent (49 g N_NH_4 m^{-3}) over the whole year.

3.5. Study case: ~~enhanced~~ optimization of microalgae production and ammonium removal efficiency over a year cycle

In this case study, the HRAP is operated with changing HRT. Higher HRT (8-day) was used in the colder months (from October to March) and lower HRT (4-day) in the warmer months (from April to September) ($HRAP_{8-4-8d}$). This strategy was selected from results obtained in the previous case studies.

Figure 10a presents simulations of X_{ALG}, X_H and TSS concentrations. X_{ALG} and microalgae/bacteria proportion (not shown, but can be deduced) changed slightly over the year in comparison by the other two case studies. X_{ALG} production was enhanced (Fig. 10b). With $HRAP_{8-4-8d}$, the production increased to 30% and 35% in $HRAP_{4d}$ and $HRAP_{8d}$, respectively.

As can be seen in Figure 10c the model prediction indicated that average removal rate of ammonium goes up to 92% (49 g N_NH_4 m^{-3}) over the whole year.

4. Conclusion

In this work the BIO_ALGAE model was validated for a long-term period using data from a pilot HRAP operating at different HRT (4 and 8 days) during the summer and winter seasons (respectively). The model accurately matched HRAP dynamics using the calibrated values of 6 parameters obtained in previous work by the authors.

BIO_ALGAE has demonstrated by means of practical study cases to be a useful tool to understand microalgae and bacteria interactions in wastewater treatment, and in particular to study the effect of different HRAP operating strategies on the relative proportion of microalgae and bacteria, biomass production, and removal of ammonium. Moreover, the model could be used to optimize biomass production.~~Moreover, the model was able to enhanced biomass production.~~

E-supplementary data of this work can be found in online version of the paper

Acknowledgements

The authors thank Jason Hale for the manuscript review. This research was supported by the Spanish Ministry of Economy and Competitiveness through the project DIPROBIO (CTM2012-37860). Alessandro Solimeno also acknowledges the FPU-AP2012-6062 scholarship provided by the Spanish Ministry of Education and Science.

References

Awuah, E., 2006. Pathogen removal mechanisms in macrophyte and algal waste stabilization ponds. Dissertation, UNESCO-IHE Institute, Delft

Bennett, N.D., Croke, B.F.W., Guariso, G., Guillaume, J.H.A., Hamilton, S.H., Anthony, A.J., Marsilli, S., Newham, L.T.H., Norton, J.P., Perrin, C., Pierce, A.S., Robson, B., Seppelt, R., Voinov, A.A., Fath, B.D., Andreassian, V., 2013. Characterising performance of environmental models. Environ Model Softw. 40:1-20

Bitog, J.P., Lee, I.B., Lee, C.G., Kim, K.S., Hwang, H.S., Hong, S.W., Seo, H.I., Kwon, K.S., Mostafa, E., 2011. Application of computational fluid dynamics for modelling and designing photobioreactors for microalgae production: A review. Comput Electron Agric. 76(2):131–147

Costache, T.A., Acién Fernández, F.G., Morales, M., Fernández Sevilla, J.M., Stamatin, I., Molina, E., 2013. Comprehensive model of microalgae photosynthesis rate. Appl Microbiol Biotechnol. 17:7627-37

Dauta, A., Devaux, J., Piquemal, F., Boumnich, L., 1990. Growth rate of four freshwater algae in relation to light and temperatura. Hydrobiologia. 207:221-226

European Union, Council Directive 91/271/EEC concerning urban wastewater treatment (1991)

Faleschini, M., Esteves, J.L., Valero, M.C., 2012. The effects of hydraulic and organic loadings on the performance of a full scale facultative pond in a temperate climate region (Argentine Patagonia). Water Air Soil Pollut. 223(5):2483-2493

Fernández, I., Acién, F.G., Berenguel, M., Guzmán, J.L., Andrade, G.A., Pagano, D.J., 2014. A Lumped parameter chemical-physical model for tubular photobioreactors. Chem Eng Sci. 112:116-129

Fuentes, J.L., Inés Garbayo, I., Cuaresma, M., Montero, Z., González-del-Valle, M., Vilchez, C., 2016. Impact of Microalgae-Bacteria Interactions on the Production of Algal Biomass and Associated Compounds. Mar Drugs. 14(5):100

García, J., Hernández-Mariné, M., Mujeriego, R., 2000a. Influence of phytoplankton composition on biomass removal from high-rate oxidation lagoons by means of sedimentation and spontaneous Xocculation. Water Environ Res. 72:230–237

García, J., Mujeriego, R., Hernandez-Marine, M., 2000b. High rate algal pond operating strategies for urban wastewater nitrogen removal. Appl Phycol. 12:331–339

García, J., Hernández-Mariné, M., Mujeriego, R., 2002. Analysis of key variables controlling phosphorus removal in high rate oxidation ponds provided with clarifiers. Water SA. 28:1–8

García, J., Green, B.F., Lundquist. T., Mujeriego. R., Hernández-Mariné. M., Oswald, W.J., 2006. Long term diurnal variations in contaminant removal in high rate ponds treating urban wastewater. Bioresour Technol. 97:1709–1715

Gujer, W., Henze, M., Mino, T., Van Loosdrecht, M., 1999. Activated Sludge Model No. 3. Water Sci Techno. 39(1):183–193

Henze, M., Gujer, W., Mino, T., Van Loosdrecht, M., 2000. Activated sludge models ASM1, ASM2, ASM2d and ASM3. IWA Scientific and Technical Report No. 9, IWA Publishing, London, UK. 2000.

Iacopozzi, I., Innocenti, V., Marsili-Libelli, S., Giusti, E., 2007. A modified Activated Sludge Model No. 3 (ASM3) with two-step nitrification–denitrification. Environ Modell Softw. 22:847-861

Khorsandi, H., Alizadeh, R., Tosinejad, H., Porghaffar, H., 2014. Analysis of nitrogenous and algal oxygen demand in effluent from a system of aerated lagoons followed by polishing pond. Water Sci Techno. 70:1–95

Krasnits, E., Friedler, E., Sabbah, I., Beliavski, M., Tarre, S., Green, M., 2009. Spatial distribution of major microbial groups in a well-established constructed wetland treating municipal wastewater. Ecol Eng. 35(7):1085–1089

Larsdotter, K., 2006. Wastewater treatment with microalgae – A literature review. Vatten. 62:31-38

Mehrabadi, A., Farida, M.M., Craggs, R., 2016. Variation of biomass energy yield in wastewater treatment high rate algal ponds. Algal Res. 15:143–151

Molina Grima, E., García Camacho, F., Sánchez Perez, J.A., Fernández Sevilla, J.M., Acién Fernández, F.G., Contreras Gómez, A., 1994. A mathematical model of microalgal growth in light limited chemostat culture. J Chem Tech Biotechnol. 61:167–173

Morris, M.D., 1991. Factorial Sampling Plans for Preliminary Computational Experiments. Technometrics. 33(2):161-174

Novak, J.T., Brune, D.E., 1985. Inorganic carbon limited growth kinetics of some freshwater algae. Water Res. 19:215–225

Oswald, W.J., Gotaas, H.B., 1957. Photosynthesis in sewage treatment. Trans Am Soc Civ Eng. 122:73-105

Oswald, W.J., 1988. Microalgae and Wastewater Treatment, in Microalgal Biotechnology, Borowitzka MA and Borowitzka LJ (eds). Cambridge University Press, New York, pp 357-94

Packer, A., Li, Y., Andersen, T., Hu, Q., Kuang, Y., Sommerfeld, M., 2011. Growth and neutral lipid synthesis in green microalgae: a mathematical model. Bioresour Technol. 102:111–7

Park, J.B.K., Craggs, R.J., 2011. Nutrient removal in wastewater treatment high rate algal ponds with carbon dioxide addition. Water Sci Technol. 63(8):1758-1764

Reichert, P., Borchardt, D., Henze, M., Rauch, W., Shanahan, P., Somlyódy, L., Vanrolleghem, P., 2001. River Water Quality Model no. 1 (RWQM1): II. Biochemical process equations. Water Sci Techno. 43(5):11–30

Sah, L., Rousseau, D., Hooijmans, C.M., Lens, P., 2011 3D model for a secondary facultative pond. Ecol Model. 222(9):1592–1603

Samsó, R., García, J., 2013. Bacteria distribution and dynamics in constructed wetlands based on modelling results. Sci Total Environ. 461–462:430–440 (2013).

Silva, H.J., Pirt, J., 1984. Carbon dioxide inhibition of photosynthetic growth of chlorella. J Gen Microbiol. 130:2833-2838

Solimeno, A., Samsó, R., Uggetti, E., Sialve, B., Steyer, J.P., Gabarró, A., García, J., 2015. New mechanistic model to simulate microalgae growth. Algal Res. 12:350-358

Solimeno, A., Samsó, R., García, J., 2016. Parameter sensitivity analysis of a mechanistic model to simulate microalgae growth. Algal Res. 15:217-223

Solimeno, A., Parker, L., Lundquist, T., García, J., 2017a. Integral microalgae-bacteria model (BIO_ALGAE): application to wastewater high rate algal ponds. Sci Total Environ. 601-601:646-657

Solimeno, A., Acién, F.G., García, J., 2017b. Mechanistic model for design, analysis, operation and control of microalgae cultures: Calibration and application to tubular photobioreactors. Algal Res. 21:236-246

Von Sperling, M., 2007. Waste stabilization ponds, IWA Pubblishing, London, Uk

Wu, X., Merchuk, J., 2001. A model integrating fluid dynamics in photosynthesis and photoinhibition processes. Chem Eng Sci. 56:3527–3538

Zhou, X., Yuan, S., Chen, R., Song, B., 2014. Modelling microalgae growth in nitrogen-limited continuous culture. Energy. 73:575-580

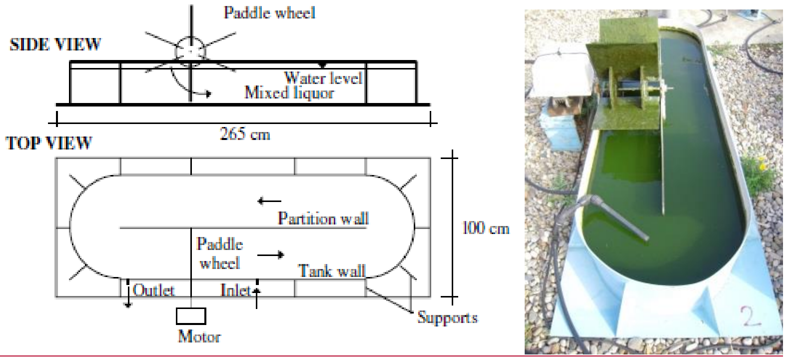

Fig. 1. Diagram of top and side views of the pilot HRAP on the left and a picture on the right. The system was located roof of the Group of Environmental Engineering and Microbiology (GEMMA) building (Universitat Politècnica de Catalunya-BarcelonaTech, Barcelona, Spain).

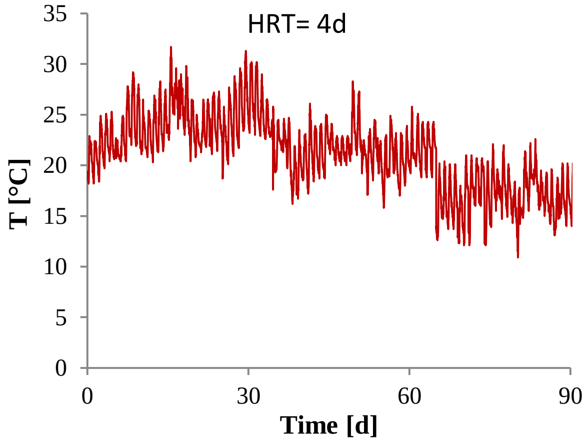

HRT= 4d

a) b)

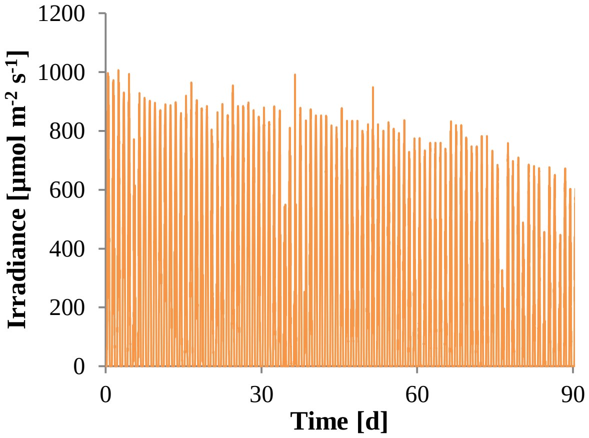

HRT= 8d

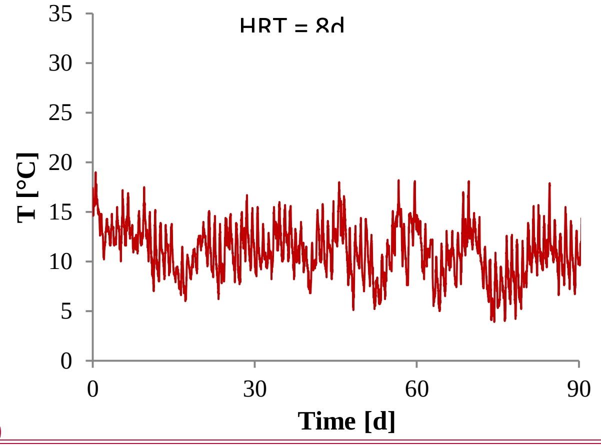

c) c)

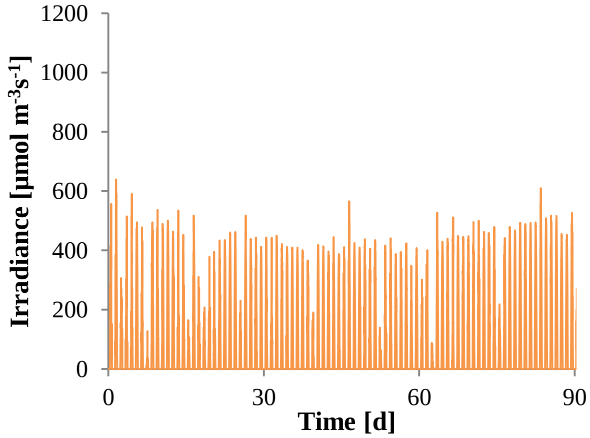

Fig. 2. Changes in air temperature and irradiance in Barcelona over Period I (July 21st – October 14th, 1993, $HRAP_{4d}$) (a, b), and over Period II (November 10th, 1993 – February 8th, 1994, $HRAP_{8d}$) (c, d). HRT in each period also shown.

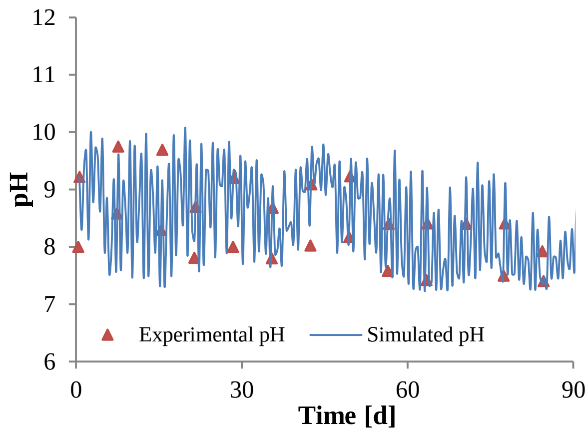
pH
12
11
10
9
8
7
6
Experimental pH
Simulated pH
0
30
60
90
Time [d]

a) b)

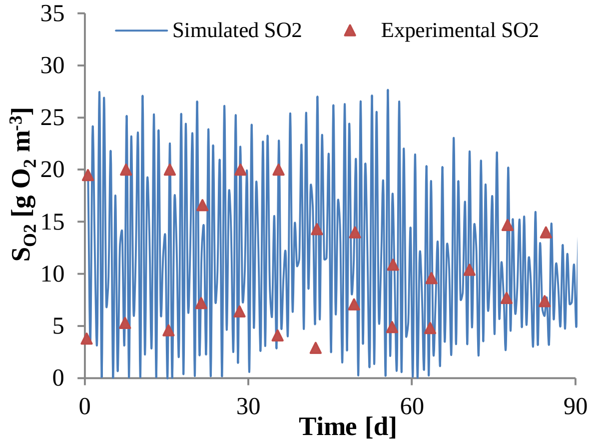
S_{O2} [g O_2 m^{-3}]
35
30
25
20
15
10
5
0
Simulated SO2
Experimental SO2
0
30
60
90
Time [d]

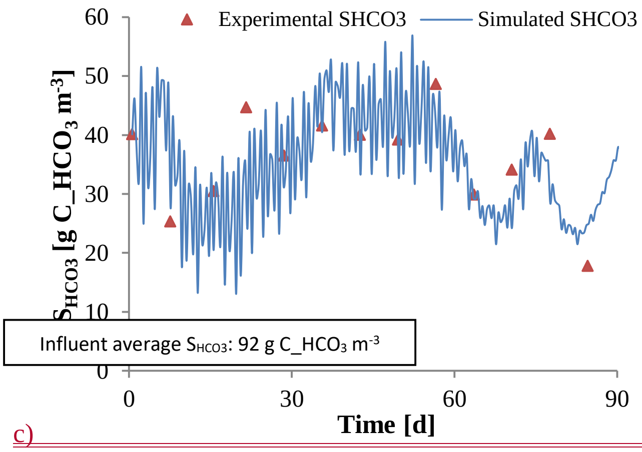

Influent average S_{NH4}: 39.8 g N-NH_4 m^{-3}

c) d)

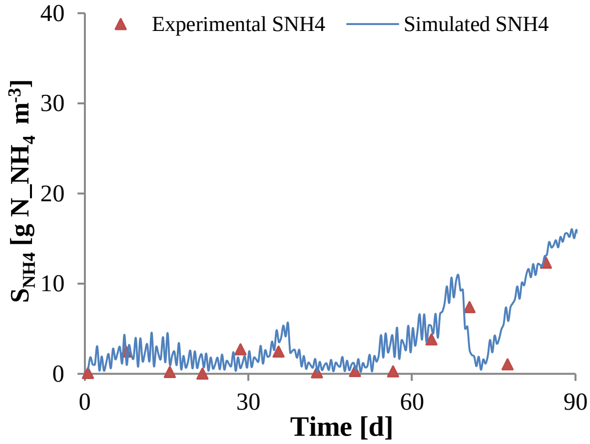

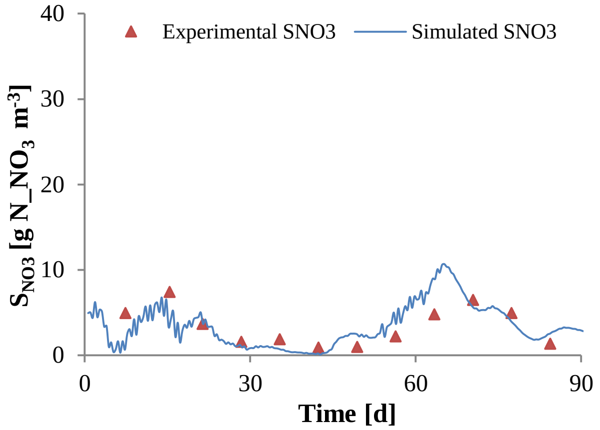
40
30
20
10
0
Experimental SNO3
Simulated SNO3
S_{NO3} [g N_NO_3 m^{-3}]
0
30
60
90
Time [d]

e) f)

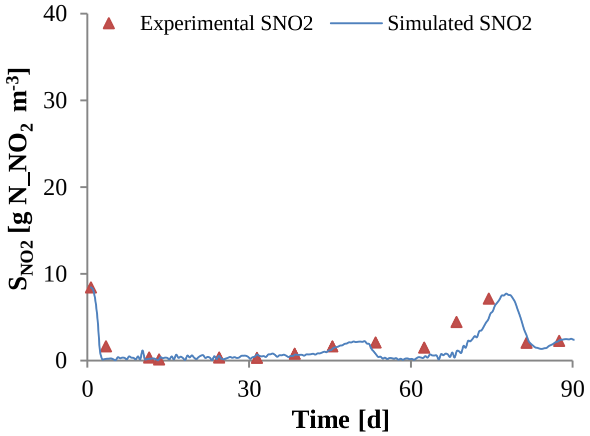
40
30
20
10
0
Experimental SNO2
Simulated SNO2
S_{NO2} [g N_NO_2 m^{-3}]
0
30
60
90
Time [d]

g)

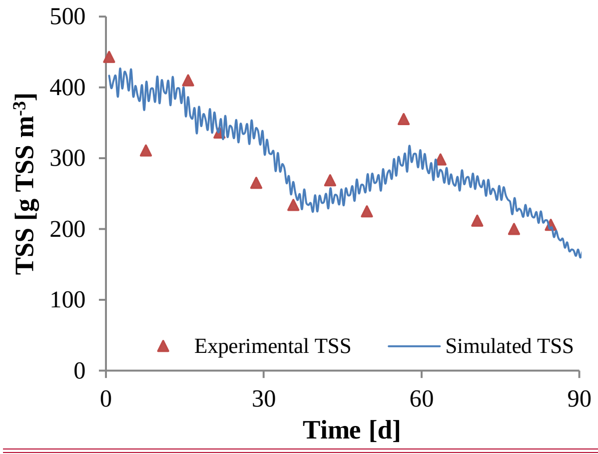

h)

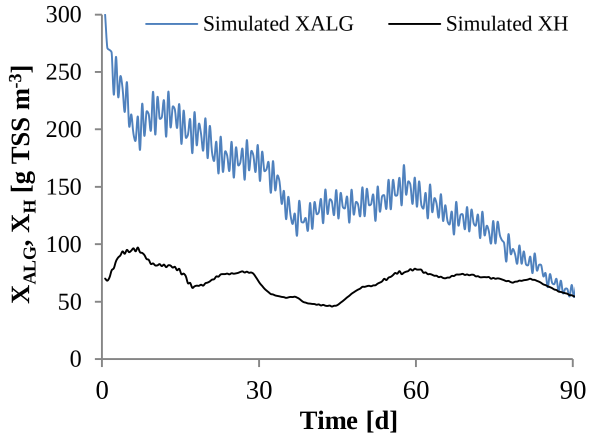

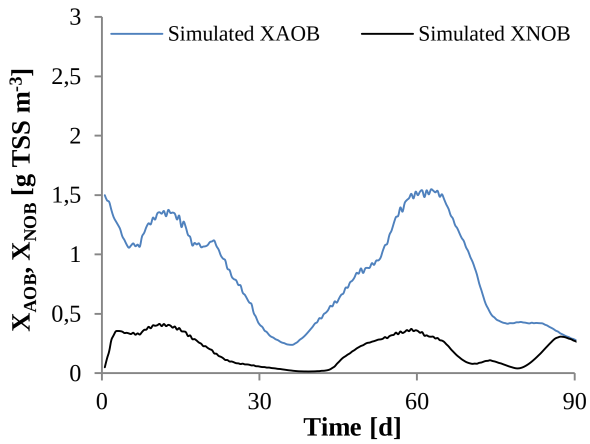

i)

Fig. 3. Changes in experimental (red triangles) and simulated (blue and black lines) a) pH, b) S_{O2}, c) S_{HCO3}, d) S_{NH4}, e) S_{NO3} f) S_{NO3}, g) TSS, h) X_{ALG} and X_H, and i) X_{AOB} X_{NOB} concentrations over the Period I (July 21st – October 14th, 1993) in the $HRAP_{4d}$. Note that in a) and b) values were measured at 9:00 AM ±1 hour and 2:00 PM ±1 hour. All other values measured at 2:00 PM ±1 hour. Higher values of pH and S_{O2}observed at 2:00 PM ±1 hour. S_{NO3} and S_{NO2} concentrations were not detected in influent wastewater.

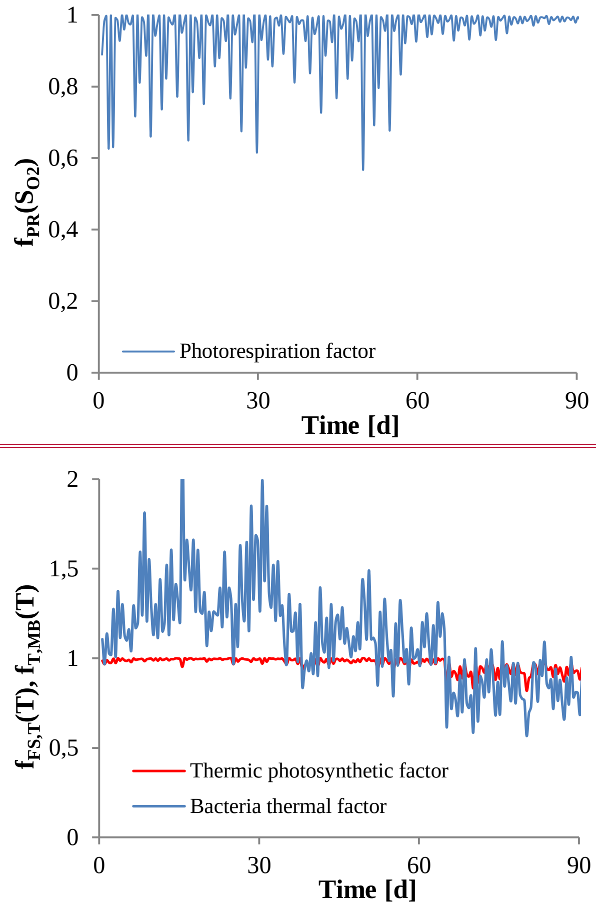

a) b)

Fig. 4. a) Changes in the values of f_{PR} (S_{O2}) and b) $f_{FS,T}$ (T) and $f_{T,MB}$ (T) factors over Period I (July 21st – October 14th, 1993) in $HRAP_{4d}$.

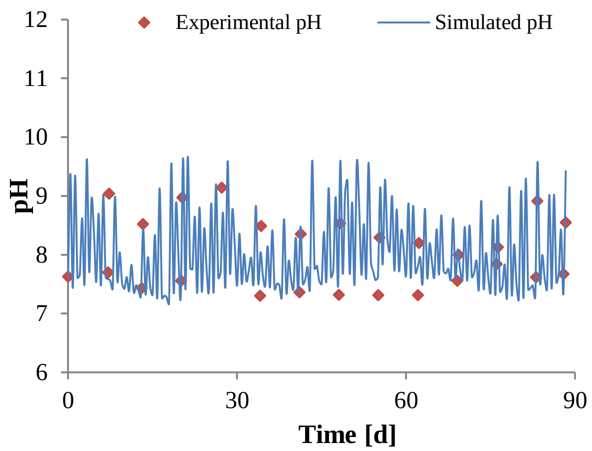
Experimental pH
Simulated pH
pH
Time [d]
12
11
10
9
8
7
6
0
30
60
90

a) b)

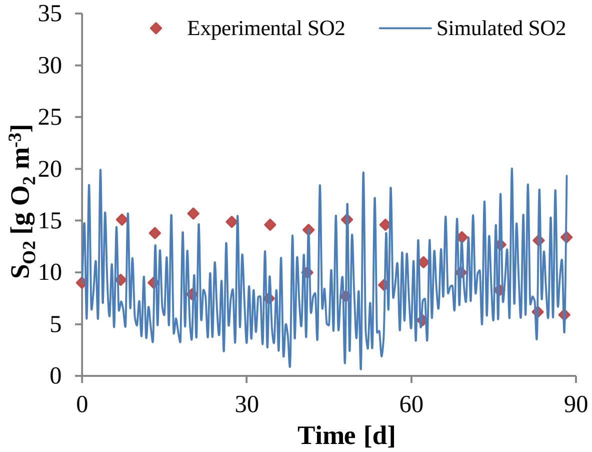
Experimental SO2
Simulated SO2
S_{O2} [g O_2 m^{-3}]
Time [d]
35
30
25
20
15
10
5
0
0
30
60
90

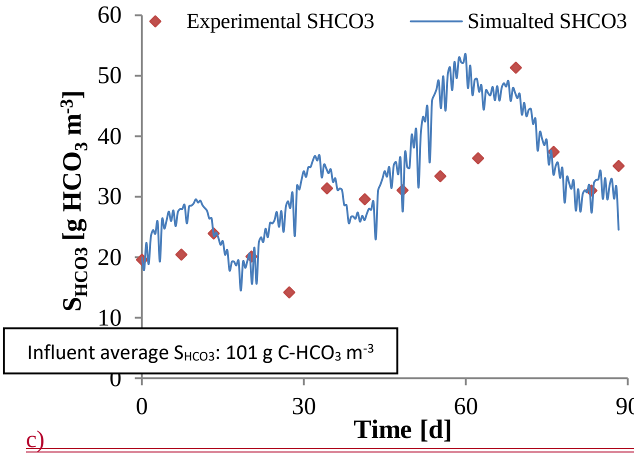

Influent average S_{NH4}: 43.7 g N-NH_4

c) d)

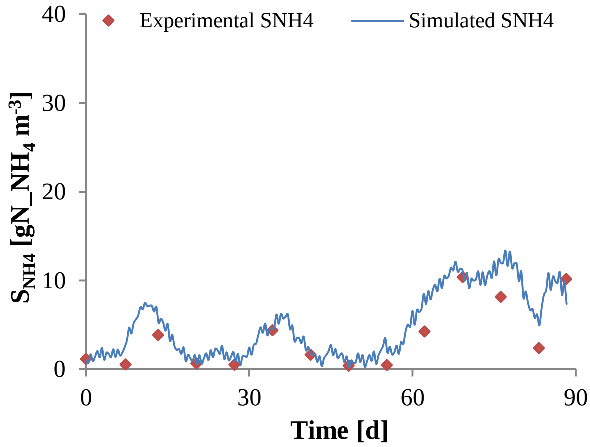

e)

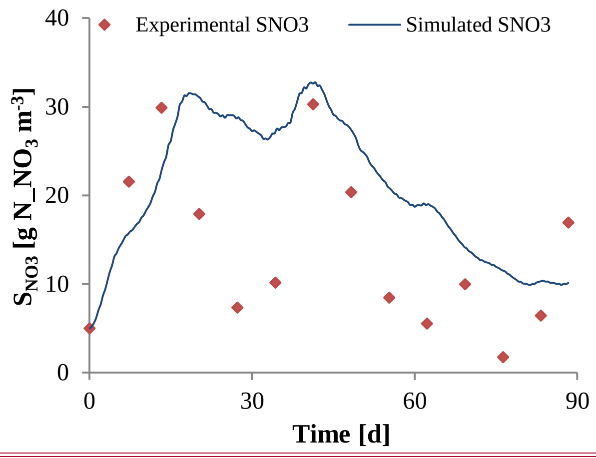
Experimental SNO3
Simulated SNO3
S_{NO3} [g N_NO$_3$ m^{-3}]
40
30
20
10
0
0
30
60
90
Time [d]

f)

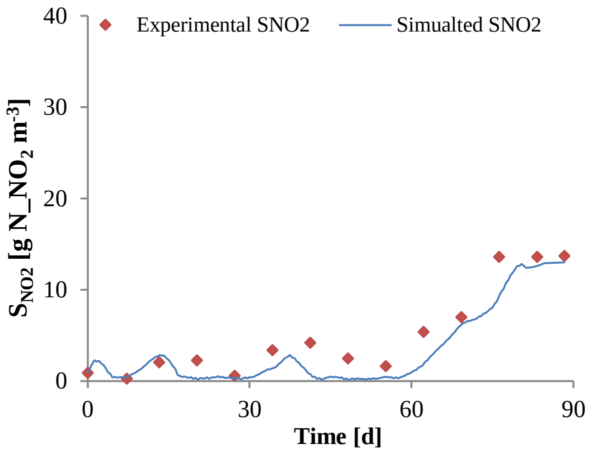
Experimental SNO2
Simualted SNO2
S_{NO2} [g N_NO$_2$ m^{-3}]
40
30
20
10
0
0
30
60
90
Time [d]

g)

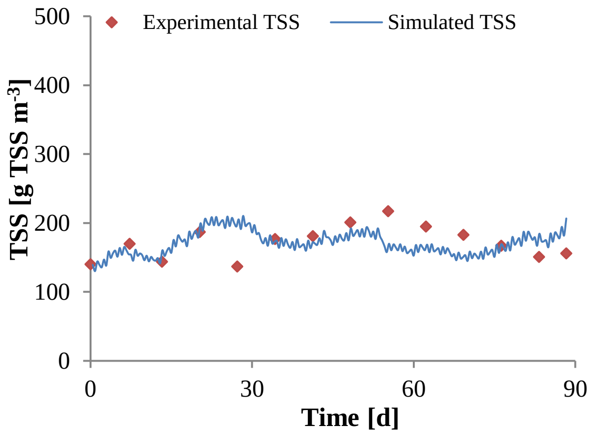
Experimental TSS
Simulated TSS
TSS [g TSS m-3]
0
100
200
300
400
500
0
30
60
90
Time [d]

h)

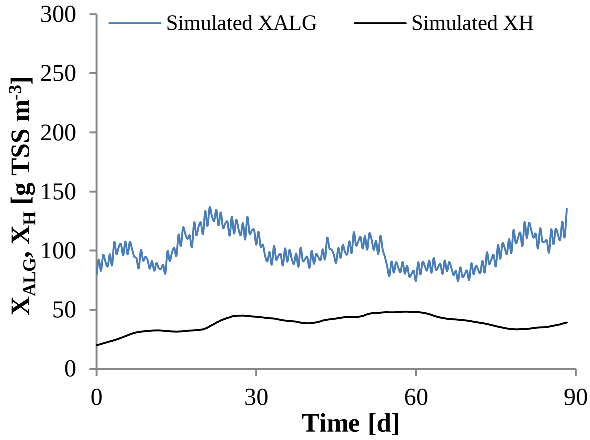
Simulated XALG
Simulated XH
XALG, XH [g TSS m-3]
0
50
100
150
200
250
300
0
30
60
90
Time [d]

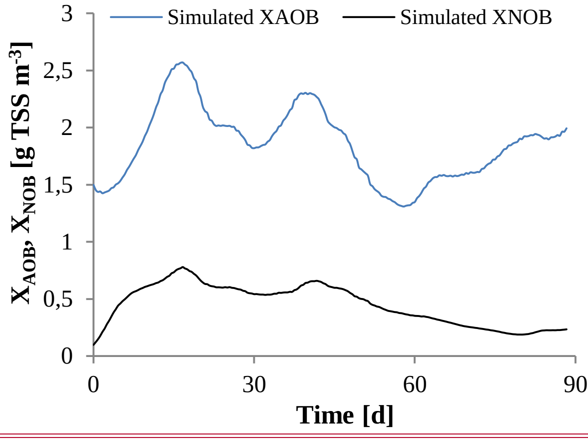

i)

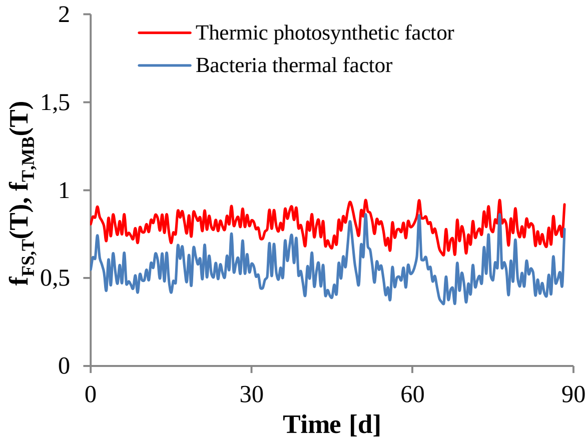

j)

Fig. 5. Changes in experimental (red diamonds) and simulated (blue and black lines) a) pH, b) S_{O2}, c) S_{HCO3}, d) S_{NH4} e) S_{NO3}, f) S_{NO2}, g) TSS, h) X_{ALG} and X_H, i) X_{AOB} and X_{NOB} concentrations and j) changes in the values of $f_{FS,T}$ (T) and $f_{T,MB}$ (T) factor over the Period II (November 10th, 1993 – February 8th, 1994) in the $HRAP_{8d}$. Note that in a) and b) values were measured at 9:00 AM ±1 hour and 2:00 PM ±1. All other values measured at 2:00 PM ±1 hour. Higher values of pH and S_{O2} observed at 2:00 PM ±1 hour. S_{NO3} and S_{NO2} concentrations were not detected in influent wastewater.

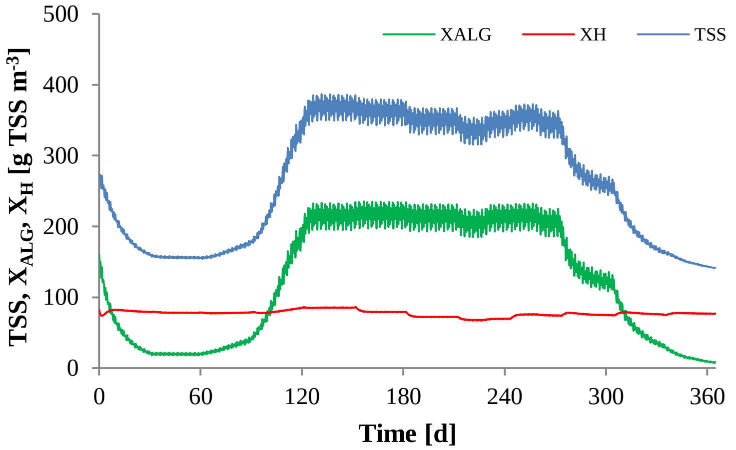

a)

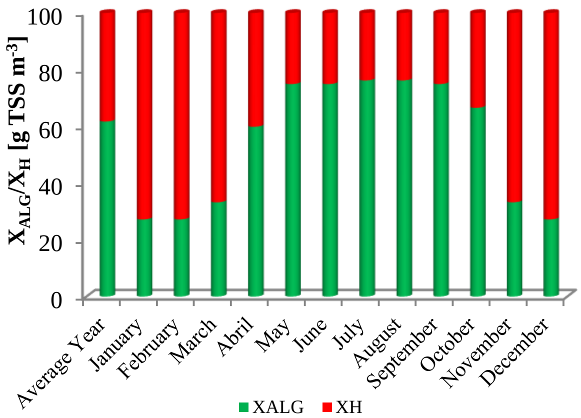

b) c)

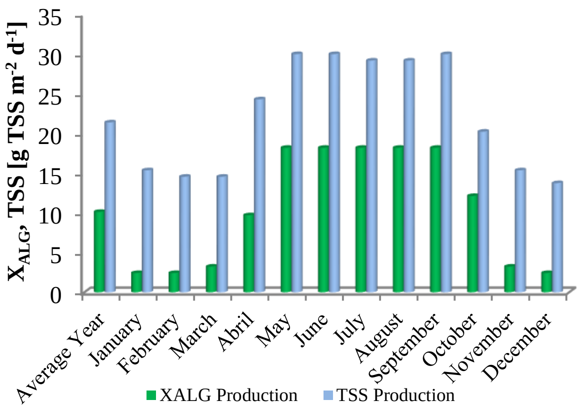

Fig. 6. a) Simulated TSS (blue line), X_{ALG} (green line) and X_H (red line) concentration over a year (from January to December) in HRAP$_{4d}$. Average annual and monthly b) X_{ALG} and X_H concentration proportion, and c) X_{ALG} and TSS in HRAP$_{4d}$.

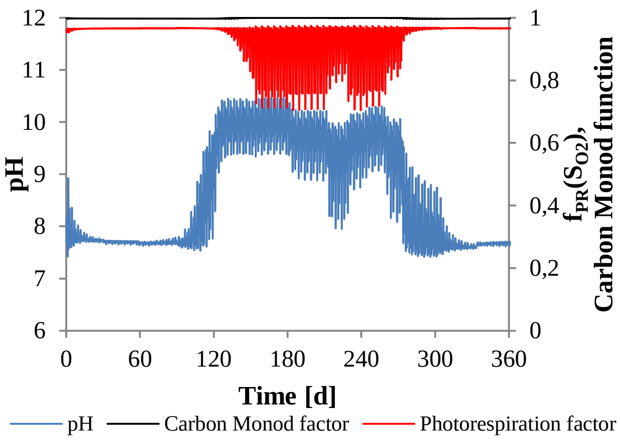

a) b)

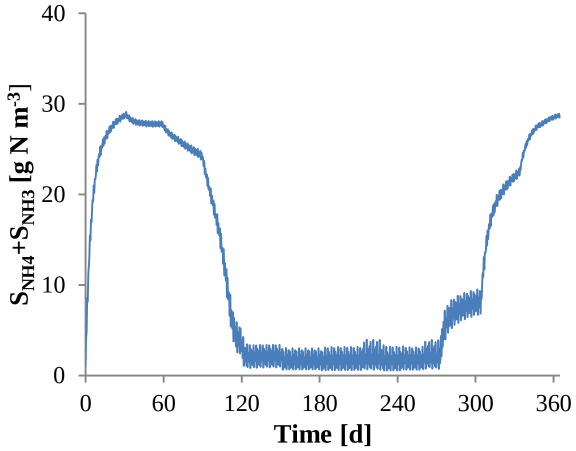

Fig. 7. Changes in a) pH, $f_{PR}(S_{O2})$ and carbon Monod function value and b) $S_{NH4}+S_{NH3}$ concentration over a year in $HRAP_{4d}$.

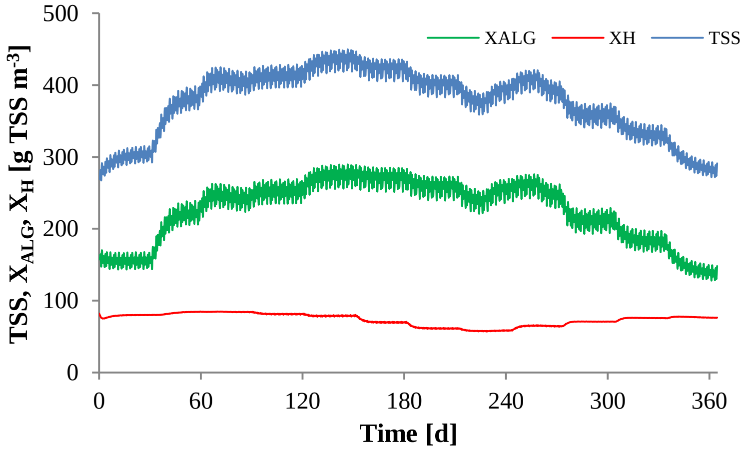

a)

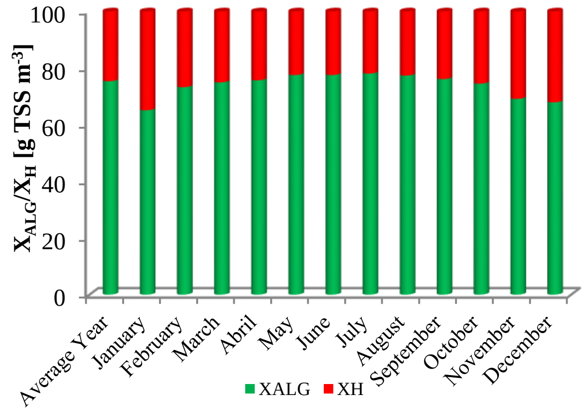

b) c)

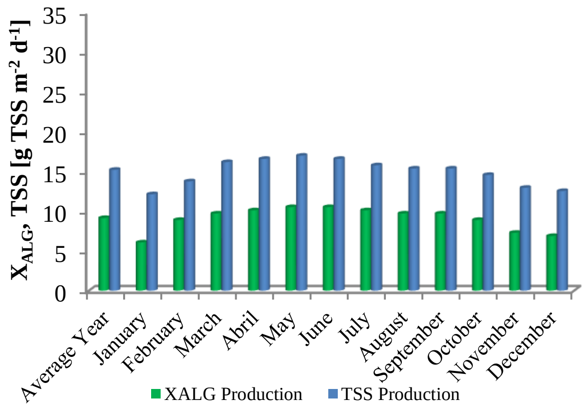

Fig. 8. a) Simulated TSS (blue line), X_{ALG} (green line) and X_H (red line) concentration over a year (from January to December) in $HRAP_{8d}$. Average annual and monthly b) X_{ALG} and X_H concentration proportion, and c) X_{ALG} and TSS in $HRAP_{8d}$.

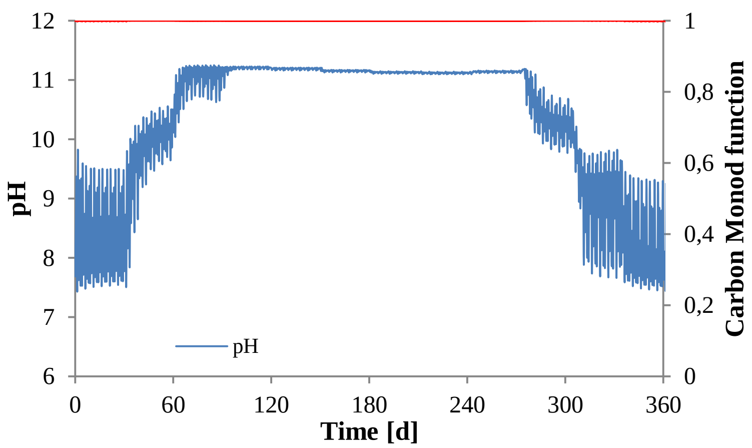

a)

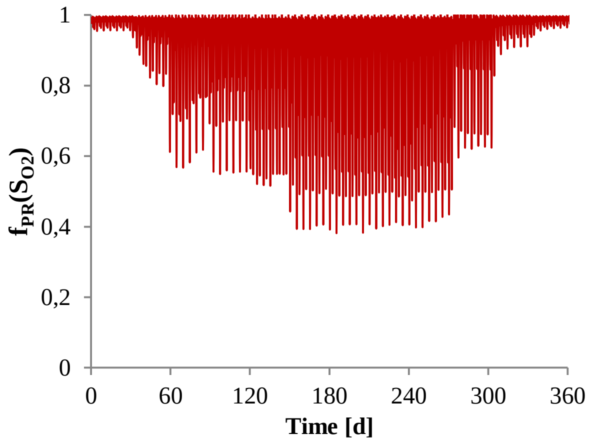

b) c)

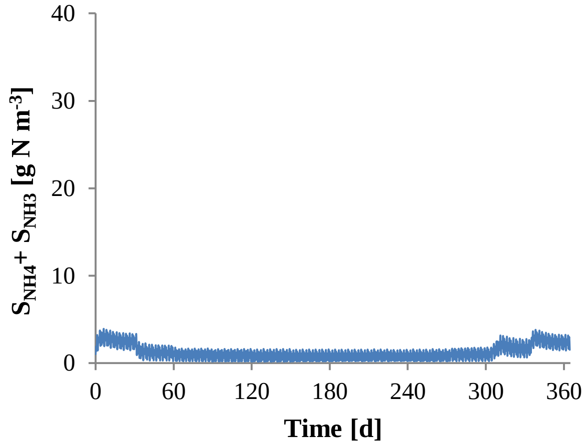

Fig. 9. Changes in a) pH value and carbon Monod function, b) (f_{PR} (S_{O2})) values and c) S_{NH4}+S_{NH3} concentrations over a year in $HRAP_{8d}$.

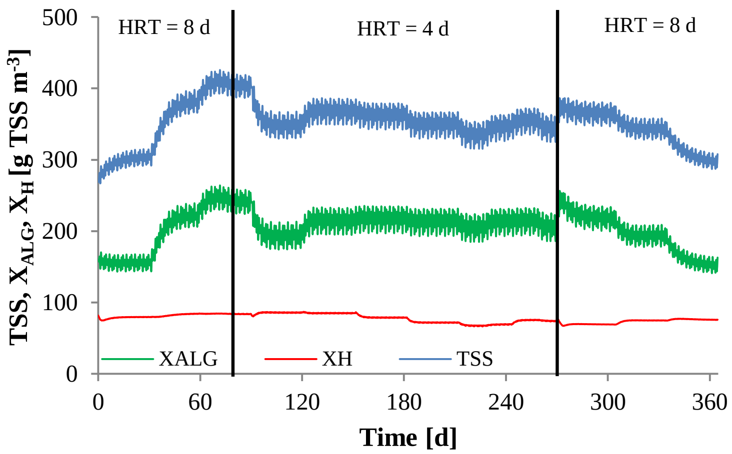

a)

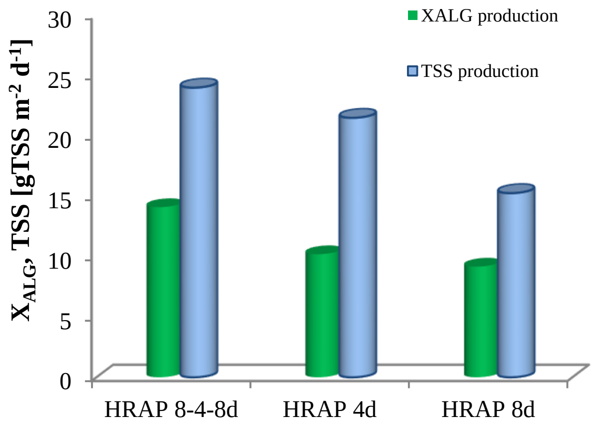

b) c)

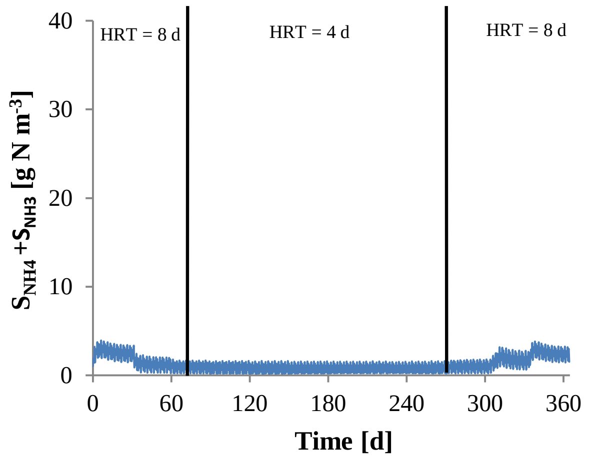

Fig. 10. a) Simulated TSS (blue line), X_{ALG} (green line) and X_H (red line) concentration over a year (from January to December) in $HRAP_{8\text{-}4\text{-}8d}$. Vertical black lines indicate HRT change. b) Comparison of average annual X_{ALG} and TSS production over a year as function of different HRT operating strategies and c) Changes in S_{NH4}+S_{NH3} concentration over a year in $HRAP_{8\text{-}4\text{-}8d}$. Vertical black lines indicate the change of HRT.